

MICROLAB NORTHWEST

7609 140TH PL. NE
REDMOND, WA 98052
PHONE: (206) 885-9419

LABORATORY REPORT

TO: Lawrence Taylor Jr., Environmental Engineer
Anchorage Air Pollution Control Agency
P.O. Box 196650
Anchorage, Alaska 99519-6650

REPORT #: 1062-94
DATE: Oct. 17, 1994

PHONE: (907) 343-4713 FAX: (907) 343-6740

SUBJECT: Source of Particles on PM10 Filters

SPECIMEN: Gamble Street Locations, Anchorage, Alaska

REFERENCE: Microlab Northwest Laboratory Reports 963-90 and 956-94

SUMMARY

Eighteen PM10 filters have been examined as part of this study spanning the time interval from April 4, 1989 to February 14, 1994. Each of these samples have been examined in detail and documented photographically as part of this analysis. Thirty-four photographs have been included as part of this report.

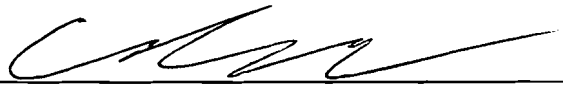
Thirteen of these samples had been analyzed in the past (see referenced reports). The results of these previous analyses have been incorporated as part of this analysis. The additional five samples provided a better characterization of the particle assemblages typical of the Anchorage area. This information has made possible a better estimation of the sources of the particles seen on the PM10 samples:

SAMPLE DATE	PM10 Loading	Assem. Ranking (%)
April 4, 1989	80 $\mu\text{g}/\text{m}^3$	Traffic, Sand
April 12, 1989	91 $\mu\text{g}/\text{m}^3$	Traffic (57%), Sand (43%)
April 22, 1989	50 $\mu\text{g}/\text{m}^3$	Traffic (100%)
Sept. 8, 1989	33 $\mu\text{g}/\text{m}^3$	Natural (78%), Traffic (22%)
April 7, 1990	152 $\mu\text{g}/\text{m}^3$	Ash (40%), Traffic (40%), Sand (20%)
April 9, 1990	188 $\mu\text{g}/\text{m}^3$	Ash (45%), Sand (28%), Traffic (27%)
April 11, 1990	260 $\mu\text{g}/\text{m}^3$	Ash (50%), Sand (30%), Traffic (20%)
July 1, 1992	47 $\mu\text{g}/\text{m}^3$	Traffic (100%)
Aug. 13, 1992	31 $\mu\text{g}/\text{m}^3$	Traffic (80%), Natural (20%)
Aug. 19, 1992	989 $\mu\text{g}/\text{m}^3$	Ash (95%), Traffic (5%)
Aug. 20, 1992	446 $\mu\text{g}/\text{m}^3$	Ash (87%), Traffic(12%), Natural (1%)
April 5, 1993	164 $\mu\text{g}/\text{m}^3$	Sand (55%), Traffic (25%), Ash (20%)
April 7, 1993	185 $\mu\text{g}/\text{m}^3$	Sand (45%), Traffic (35%), Ash (20%)
April 7, 1993	Collocated Sample	Sand, Traffic, Ash
April 8, 1993	171 $\mu\text{g}/\text{m}^3$	Sand (40%), Traffic (38%), Ash (22%)
April 9, 1993	162 $\mu\text{g}/\text{m}^3$	Sand (40%), Ash (30%), Traffic (30%)
Nov. 4, 1993	161 $\mu\text{g}/\text{m}^3$	Traffic (48%), Sand (32%), Ash (20%)
Feb. 14, 1994	242 $\mu\text{g}/\text{m}^3$	Sand (40%), Traffic (36%), Ash (24%)

The samples from April 1990 were strongly influenced by the Mount Redoubt ash fall. By 1992 no recent ash was evident in the samples until the eruption of Mount Spur, August 18, 1992. The large quantity of Mount Spur ash that fell on Anchorage has resulted in its persistent presence in the samples since that time. The Mount Spur ash in the April 1993 samples exhibits evidence of weathering, a process involved in incorporating the ash fall into the natural soil. The main contributors to the particle loading in April 1993 and since that time have been sand on the road and traffic debris.

Thank you for this opportunity to be of service. If I can provide any further assistance please contact me.

Signed: _____



E. R. Crutcher, Consultant

INTRODUCTION

Eighteen PM10 filters have been examined as part of this study spanning the time interval from April 4, 1989 to February 14, 1994. The full series is listed below:

SAMPLE DATE	LOCATION	PM10 Loading
April 4, 1989	Gamble St.	80 $\mu\text{g}/\text{m}^3$
April 12, 1989	Gamble St.	91 $\mu\text{g}/\text{m}^3$
April 22, 1989	Gamble St.	50 $\mu\text{g}/\text{m}^3$
Sept. 8, 1989	ERPG A	33 $\mu\text{g}/\text{m}^3$
April 7, 1990	Gamble St.	152 $\mu\text{g}/\text{m}^3$
April 9, 1990	Gamble St.	188 $\mu\text{g}/\text{m}^3$
April 11, 1990	Gamble St.	260 $\mu\text{g}/\text{m}^3$
July 1, 1992	Gamble St.	47 $\mu\text{g}/\text{m}^3$
Aug. 13, 1992	Gamble St.	31 $\mu\text{g}/\text{m}^3$
Aug. 19, 1992	Gamble St.	989 $\mu\text{g}/\text{m}^3$
Aug. 20, 1992	Gamble St.	446 $\mu\text{g}/\text{m}^3$
April 5, 1993	26C	164 $\mu\text{g}/\text{m}^3$
April 7, 1993	26A	185 $\mu\text{g}/\text{m}^3$
April 7, 1993	26A	Collocated Sample
April 8, 1993	26C	171 $\mu\text{g}/\text{m}^3$
April 9, 1993	26D	162 $\mu\text{g}/\text{m}^3$
Nov. 4, 1993	26C	161 $\mu\text{g}/\text{m}^3$
Feb. 14, 1994	26C	242 $\mu\text{g}/\text{m}^3$

Three additional samples were received as reference standards: Mount Redoubt ash fallout from the eruption of December 21, 1989; MOA #1, ash collected in a square meter rain collector that was in place during the volcanic ash fallout from Mount Spur of August 18, 1992; and MOA Sand #1, sand from the stock pile used on the roads in Anchorage during the winter of 1994. The reference samples were ground in a mortar and pestle and then mounted in 1.539 Melt Mount for evaluation.

The purpose of the analysis was to determine the role of volcanic ash in the elevated levels of PM10 loading experienced in the Anchorage area during the years from 1990 through 1994 and to clearly document the evidence upon which those conclusion were based. The photographs included as part of this report are provided to demonstrate how specific particle types are distinguished. The documented procedures indicate step by step how the analysis of individual particles becomes a quantitative analysis of contributions from specific sources. The question of secondary emission or resuspension is an issue related to these samples and will be addressed in this report in the Results section.

METHODS

This section is divided into four sections: Sample Preparation, Qualitative Analysis, Assemblage Analysis, and Quantitative Image Analysis. Each section includes a

description of the procedures followed for this study.

Sample Preparation

Samples of each of the filters were prepared by placing a section of the loaded filter from near the center of the filter, particle side down, onto a Melt Mount 1.539 coated microscope slide. The filter section was approximately 3/4 by 1 1/2 inches. Smaller sections of heavily loaded filters were used to prevent overloading the mounting medium. The filter was gently pressed into the Melt Mount at ambient temperature, approximately 70° Fahrenheit, and then removed. The slide with the sample was then heated to approximately 230° Fahrenheit and a 0.9 by 1.5 inch coverslip was added.

To assure that this procedure produced a representative sample a section of the entire filter thickness was mounted in a liquid with a refractive index nearly matching the refractive index of the glass fiber in the filter. This made the glass fiber invisible and allowed for an examination of the particle distribution through the filter mat. The particle types and distribution seen in this mount was compared to the mount prepared for detailed analysis. The distribution of particle types was found to be essentially the same in each case. The full filter thickness mount could not be used effectively for the more detailed analysis due to the optical depth of the mount, the heavy loading of the filters of interest, and the agglomeration of particles on the filter due to the effects of channeling in the filter.

Qualitative Analysis

Each sample was examined qualitatively with a Nikon Optophot Pol microscope to determine the types of particles and particle assemblages represented (see below for Assemblage Analysis). The microscope was configured to use transmitted circular polarized light for photographic documentation. Circular polarized light maximizes the polarized light effect for photographic documentation and for image analysis but at the expense of losing detailed information on the exact optical properties of the particles documented. Full characterization of the particles required the use of crossed linear polarized light, transmitted oblique and reflected oblique, transmitted and reflected darkfield, and phase contrast illumination. Particle shape, refractive indices relative to the 1.539 refractive index mounting medium, extinction position, crystal twinning, color, internal structure, external texturing, absorptive index, birefringence, and dispersion characteristics were used in the qualitative analysis. The properties exhibited by specific particles were compared to standards of known materials and to table values in reference books or to references on source modified or source specific assemblages of particles. The lists of particle types generated was then used to characterize sources by assemblage analysis and to select image analysis criteria for the quantitative analysis.

Assemblage Analysis

The technique of assemblage analysis is based on the fact that any given source generates a variety of particle types that are characteristic of that source. Often the particle types are not individually unique to that source but the combination of particle types, their

relative quantity, size distribution, and surface characteristics indicate that the source in question is or is not a significant contributor to the site in question. A subdivision of this type of analysis is the technique called tracer analysis. In tracer analysis a unique particle type characteristic of a specific source is used to indicate the impact of that source at the collection site. This unique particle type may be a small fraction of the total particulate matter created by the source but it is unique to that source. In such a case low levels of the tracer particle population in a sample might indicate the total contribution of its source at the collection site was quite high.

In the violation samples that constituted this study four assemblages dominated the particle populations: Fresh Mount Redoubt Ash (Photographs 1 and 2), Fresh Mount Spur Ash (Photographs 3 and 4), Traffic Debris (Photographs 10, 11, and 17), and Road Sand (Photographs 5, 6, 7, and 8). The natural background assemblage of minerals and biological materials was most evident on the filters with very low total loading (Photographs 9, 18, and 20) though even there they were mixed with traffic debris. A few other assemblages were also present. The rationale for the assemblages as they appear below is presented in the Results section of this report. The assemblages are characterized as follows:

Fresh Mount Redoubt Ash: High glass content ash. Iron concentrated in larger iron rich mineral particles resulting in a light colored ash of predominantly transparent glass and minerals with a few larger black iron oxide particles. Feldspar pinocoids were common. Most crystals were covered with frothy glass foam. The refractive index of the glass is well below the 1.539 of the mounting medium

Fresh Mount Spur Ash: Iron dispersed as very fine iron rich minerals through the glass phase of the ash resulting in a dark colored ash. Microliths (small elongated crystals) were commonly dispersed in the glass phase particles. The feldspar crystals were more equant in shape. The glass phase was less frothy and formed more globular structures than that seen in the Mount Redoubt Ash assemblage suggesting a higher viscosity at the time of emission. The refractive index of the glass is nearly the same as that of the mounting medium, 1.539.

Traffic Debris: Black, irregular, tapered cylinders, transparent at thinnest edges, with small inclusions of mineral grains, and high fractal texture characterizes tire wear, a tracer particle for traffic debris. Tire wear need not always be tapered cylinders (see Photograph 30) Tire wear is distinguished from black volcanic glass by the high fractal surface, and the associated mineral inclusion visible only at the edges of the tire wear particles. Tire wear is only a small part of the traffic debris assemblage. Asphalt containing clumps of minerals (see Photographs 10, 19, 26, and 30), natural minerals, rust, wear metals, cenospheres, and soot are also part of the assemblage.

Road Sand: A mixture of natural minerals including igneous, metamorphic, and sedimentary materials comprise the sand used on the roads during the winter of 1993/1994. The igneous forms were primarily andesidic,

the same general types as those minerals generated by the eruptions of Mount Redoubt and Mount Spur. The glass phase ranged from lower in refractive index than the mounting medium, 1.539, to a matching refractive index. The igneous minerals are the most common types of minerals found in the road sand. The minerals are eroded exhibiting no fragile structures. Water worn minerals are evident as part of the sedimentary minerals as are foraminifera (calcium carbonate shell casts of marine life). The foraminifera are a tracer particle for this type of road sand. Foraminifera fragments constitute a small part of the total road sand but they are not found in volcanic ash or as a significant part of the natural background assemblage.

Natural Background: Pollens, spores, plant parts, fungal mycelium, diatoms (silica based shell casts), insect parts, and natural minerals constitute the natural background. The natural minerals are small, equant or tabular grains.

Other Assemblages: Flyash is present at low levels in some samples indicating incineration sources. Some of the minerals present are possibly the result of construction activities. No information on construction activities or samples of deeper soils from construction sites is available.

Natural minerals are a part of every one of these assemblages. Specifically, feldspar minerals are a major part of all of the ash samples and the road sand sample, and are minor constituents in the traffic debris, natural background, and other assemblages. Feldspar particles are the major particle type in all of the violation samples. The identification of feldspar in these samples is of little value unless the specific origin of the feldspar can be determined. That is the purpose of assemblage analysis.

Quantitative Image Analysis

The image analyzer used was an Olympus Cue II analyzer. It is sensitive to 254 gray levels. The image analyzer quantifies objects detected in the field of view that are brighter or darker in terms of gray level than the background illumination. The microscope illumination system is used to create a condition in which the particles of interest are brighter or darker than the gray level of the background. A preliminary step in this process is to determine how particles of interest in such a complex sample can be reduced to discriminations based primarily on brightness. For these samples opaque particles, crystalline particles, and volcanic glass particles formed population of interest and they could be easily differentiated based on brightness using the appropriate type of microscope illumination. The assemblages in this study were distributed across these three optical properties as shown in Table 2 and Table 3.

Although the Natural assemblage and the Mount Redoubt assemblage appeared similar the isotropic particles in the Natural assemblage were all biological materials and in the Mount Redoubt assemblage they were volcanic glass particles. These two were easily differentiated on the basis of semi-quantitative qualitative analysis (see Results section).

	OPAQUES	CRYSTALLINE	ISOTROPIC
Mount Redoubt	20%	50%	30%
Mount Spur	30%	50%	20%
Traffic Debris	77%	18%	5%
Road Sand	10%	80%	10%
Natural	10%	40%	50%

Table 1: Distribution of Assemblages by Optical Properties

	OPAQUES	CRYSTALLINE	ISOTROPIC
Mount Redoubt	magnetite, black glass	feldspars, pyroxenes, other crystalline minerals.	volcanic glass
Mount Spur	magnetite, black glass	feldspars, pyroxenes, other crystalline minerals.	volcanic glass
Traffic Debris	tire wear, wear metal, cenospheres, soot, asphalt, opaque road minerals	crystalline road minerals	isotropic road minerals
Road Sand	black glass, magnetite	feldspar, pyroxenes, quartz, shell fragments, limestone, mica, amphibols, etc.	volcanic glass, garnet, etc.
Natural	black spores, black biologicals, magnetite, char	plant fibers, crystalline mineral	pollens, spores, diatoms, epithelial materials

Table 2: Distribution of Particle Types by Assemblage and Optical Properties

For this analysis three basic illumination configurations were used. Transmitted darkfield illumination was used to quantify the total particle population of a field of view. With this type of illumination all particles, even the black opaque particles as a result of light reflecting from their edges, show up as brighter than the black background. Glass fibers from the filter interfered with some fields of view and had to be manually edited from the detected image prior to analytical processing.

Transmitted circular polarized light was used to quantify the crystalline materials present. Circular polarized light results in all crystalline materials exhibiting their maximum interference color (brightness) while all non-crystalline particles remain black like the background. An objective with a numerical aperture of 0.65 was used for the analysis so that even when a crystal's alignment was such that its optic axis or bisectorix was parallel to the optical path of the microscope the particles would appear bright.

The opaque particle population was quantified using transmitted off crossed circular polarized (crossed + 10 degrees) illumination to minimize interferences from light scattering particles common in volcanic ash. With this configuration the light scattering particles created sufficient depolarization to appear brighter than the background while the opaque particles remained much darker than the background.

Each field of view was analyzed using each technique before the slide was moved to a new field of view. This assured identical fields of view for each step in the analysis. Ten fields of view were analyzed per mounted sample. All measurements were recorded as the percent area covered for each field of view (see attached tables). The darkfield image was higher in area than the actual area of the total particulate matter due to the enhanced halo glow of the particles but the same setting was used for each analysis so that the data is normalized to that setting. The relative contribution of the different types of particles in a given sample was determined based on the total fraction they represented of the total particle area for that sample. Finally semi-quantitative information was used to assess the assemblage contributing to the total loading.

Not all samples have been analyzed using quantitative image analysis. In the Results section the analytical methods used for the analysis of each filter will be presented with the results of the analysis for that filter.

RESULTS

The Mount Redoubt ash sample standard was collected at the Anchorage airport on December 21, 1989. Photographs 1 and 2 illustrate some of the basic characteristics of this ash. Photograph 1 is at a magnification of 237X (1/4in. = 27 μ m). The particles that are white or colored in this photograph are primarily feldspar crystals (A) with a few pyroxenes (B). The feldspar has refractive indices slightly higher than that of the mounting medium (1.539) as is indicated by the thin boundary between the particle and the mounting medium where the feldspar is not covered by volcanic glass (C). The volcanic glass particles are all those particles that have about the same color as the background (D). The glass contains gas bubbles, smaller crystals, and black inclusions. In the upper center and center right are two glass foam particles (E). The dark boundary at the edge of the glass particles in this mounting medium indicate that the refractive index of the glass is significantly lower than the mounting medium. Along the upper right side of this photograph is a dark centered glass particle with a few yellow crystal inclusion along its right side (F). The yellow inclusions are pyroxene crystals. The black is magnetite, iron oxide. This eruption contained a large fraction of rectangular crystals of feldspar covered with frothy glass foam. Two examples of this feature can be seen in the center of the photograph (G). Both rectangular crystals can be seen to be covered with a layer of glass that is quite jagged and fragile. The dark boundaries between the rectangular feldspar particles and the glass that surrounds them is due to the relatively large difference between their refractive indices. The small black particles distributed through the field are magnetite grains (H). Most of the iron

in this ash is concentrated in these relatively large single grains.

Photograph 2 shows the Mount Redoubt ash at a magnification of 950X (1/4in. = 6.7 μ m). The frothy foam characteristic of the glass is evident in the form of these small fragments, especially the medium sized particle near left lower center (A). The thin plates of glass are fragments of bubble walls. Many of the particles exhibit ridges that mark the boundary where three bubbles met (see the two near center, location B in the photograph, one just above center and one just below). Notice that the glass is clear for the most part and that the iron is separated in individual black particles at this magnification (C).

Photograph 3 shows the particles from the August 18, 1992 eruption of Mount Spur at a magnification of 237X (1/4in. = 27 μ m). Notice the darker appearance of the ash. This is due to very fine particles of iron oxide dispersed through the volcanic glass (A). The dark volcanic glass has a refractive index that is just slightly below that of the mounting medium as indicated by the thin boundary around these particles (B). The lighter particles in the photograph are feldspar (C).

Photograph 4 shows the Mount Spur ash at a magnification of 950X (1/4in. = 6.7 μ m). Much of the Mount Spur volcanic glass is full of microliths, small elongated crystals (A). Note that the glass matrix is nearly invisible due to the close match of the refractive index of the mounting medium to that of the glass (B). Much of the glass is iron oxide filled (C). Free magnetite (iron oxide) particles are also present (D).

Photograph 5 is a sample of the sand used on the roads in Anchorage during the winter of 1994. This photograph is at a magnification of 95X (1/4in. = 67 μ m). Most of the bright particles in the field of view are feldspar crystals (A) but quartz (B), pyroxenes (C), magnetite (D), and clay (E) particles are present. Right of the photograph center at location F is a foraminifera casing (shell). Glass fragments are common as smaller particles (G). Most of the particles in this field of view are too large to be captured in a PM10 collector but they are representative of those particles that would be crushed by traffic on the road and could then become airborne as finer fragments.

Photograph 6 is road sand at a magnification of 237X (1/4in. = 27 μ m). It contains a large feldspar particle (A) and a particle of picrolite (B), the radiating particle at the center of the photograph. When crushed the picrolite produces small lath-like particles such as that shown in photograph 34(B).

Photographs 7 and 8 shows the crushed road sand particles at a magnification of 950X (1/4in. = 6.7 μ m). In both photographs significant amounts of glass particles are present (A). The glass has refractive indices below that of the mounting medium. This distinguishes this glass from that seen in the Mount Spur material. Shell fragments are also a common material present in these photographs (B). Near the center of photograph 7 is a white elongated quartz particle with rounded ends (C). This indicates a water worn mineral grain and not a product of volcanic emission. A clay particle can be seen in the upper left of photograph 7 (D). The road sand is a complex deposit consisting of primarily andesitic volcanic material with additional materials typical of a marine sedimentary deposit. The marine aspect with the associated shell material and the sedimentary materials of non-

andesitic volcanic and other minerals help to discriminate the sand material from the recent ash fall material.

One of the natural background particle assemblages in the Anchorage area is illustrated in photograph 9. Photograph 9 is the particulate matter collected on September 8, 1989 at site ERPG A. The loading on this filter was only $33 \mu\text{g}/\text{m}^3$ and consisted largely of moss, fern, and mold spores (A). Rounded natural minerals (B) are present at lower levels of loading on the filter. This photograph was taken at a magnification of 950X ($1/4\text{in.} = 6.7\mu\text{m}$). This was the only sample to be so dominated by this spore assemblage.

Photograph 10 was from a filter collected on April 4, 1989 at a Gamble Street site and was photographed at a magnification of 237X. The glass fiber in this photograph is from the filter mat. At this magnification a number of particles can be seen to illustrate the typical particle population. This is a typical traffic debris assemblage including asphaltic particles (A), numerous tire wear particles (B), and weathered and rounded minerals of volcanic origin (C). The asphaltic particle in the upper right of the photograph consists of minerals held together with asphalt. The asphalt is soluble in the mounting medium and so has darkened the mounting medium adjacent to the particle. This type of particle is a tracer particle unique to asphaltic concrete typical of road surfaces. The tire wear particles are the elongated black cylinders tending to taper at the ends and are of various sizes in this photograph. Most of the black particles in this field of view are tire wear particles. A few cenospheres (lacy, spherical soot particles at location D) from diesel engine exhaust are also present as another typical traffic debris particle. The brighter particles in the field are primarily volcanic minerals though they lack the sharp features that are associated with fresh, unweathered volcanic ash. Shell and other particles associated with road sand are present so much of the volcanic material probably belongs to the road sand assemblage. It had been three years since the last volcanic eruption (Mount St. Augustine, January 25, 1986). The particle loading on this filter was $80 \mu\text{g}/\text{m}^3$ and is a typical traffic debris assemblage.

Photographs 11 and 12 are from the filter dated April 12, 1989. The loading on that day was $91 \mu\text{g}/\text{m}^3$. Photograph 11 was taken at a magnification of 475X ($1/4\text{in.} = 14\mu\text{m}$). Photograph 12 is the upper left section of photograph 11 seen at a magnification of 950X ($1/4\text{in.} = 6.7\mu\text{m}$). Just as in the sample from April 4, 1989 this is a traffic debris and road sand assemblage but with less road sand than in the sample from the 4th; tire wear (A) and rounded minerals (B) dominate. The April 22, 1989 sample has very little road sand type minerals. The April 22, 1989 and the July 1 1992 samples were used as standards for the normal traffic debris assemblage at this site.

Photographs 13 and 14 are from the filter dated April 9, 1990 and both are at a magnification of 950X ($1/4\text{in.} = 6.7\mu\text{m}$). The suspended particulate loading on this date was $188\mu\text{g}/\text{m}^3$. The traffic debris and the road sand assemblages are evident but there is an even greater loading of new volcanic ash. The date of this filter is about three months after the eruption of Mount Redoubt (see Photographs 1 and 2). Photograph 13 shows two large tire wear particles in the center of the frame (A). There are small rounded minerals (B) present as well as rust particles (C) but there is also fine fragile particles of volcanic glass (D). Photograph 14 is dominated by the fresh volcanic ash particles of sharp glass (A) and

large grains of magnetite (B).

Photographs 15 and 16 are from the filter dated April 11, 1990. The suspended particle loading had increased significantly over the sample collected on the 9th to $260\mu\text{g}/\text{m}^3$. With this increase the amount of fresh Mount Redoubt ash also increased. In photograph 15 a large feldspar pinicoid crystal coated with volcanic glass can be seen in the center of the picture (A). This particle is typical of the structures seen in the Mount Redoubt standard sample shown in photograph 1. Photographs 15 and 16 are at a magnification of 950X ($1/4\text{in.} = 6.7\mu\text{m}$), four times the magnification of photograph 1 but the same as that in photograph 2. Photograph 16 is another field of view in this sample and is dominated by glass foam fragments (A).

Photographs 17 through 21 illustrate the particle assemblage at the Gamble Street site just prior to the eruption of Mount Spur. This sample was collected on August 13, 1992 and Mount Spur erupted on August 18, 1992. The loading on this filter indicated a suspended particle loading of only $31\mu\text{g}/\text{m}^3$. This sample is a mixture of the natural background assemblage and of the road debris assemblage. Photograph 17 was taken at a magnification of 475X ($1/4\text{in.} = 14\mu\text{m}$), and shows one part of the typical particle population on this filter. This field is dominated by traffic debris; tire wear (A), and asphalt containing particle (B), and a cenosphere (C) but it also contains a moss spore (D). Photographs 18 through 21 are all at a magnification of 950X ($1/4\text{in.} = 6.7\mu\text{m}$). Photograph 18 shows two well rounded mineral grains (A) and a fern spore (B). This field is consistent with the natural assemblage though the rounded minerals could also be from the traffic debris assemblage. Photograph 19 is a classic asphaltic concrete road debris particle (A). Photograph 20 is nearly a classic natural background assemblage of spores (A), a rotted wood fiber (B), mold mycellium (C), and a mica flake (D) with only one traffic debris particle; a tire wear particle (E). Photograph 21 shows a rust particle (A) and a spore (B). Rust is a mixture of iron oxides and hydroxides that typically are cryptocrystalline (polycrystalline with each crystallite very small and with an orientation independent of its neighbors). The particle in photograph 21 is typical of a highly oxidized rust particle but its cryptocrystalline nature results in an averaging of its optical properties and prevents the particle from exhibiting the properties of hematite though stoichiometrically it is very close to that composition. This is typical of corrosion generated iron oxide, rust. This is quite different from the large single crystal of hematite that can grow in magma as shown in photograph 22 from a filter collected during the eruption of Mount Spur (A).

Photographs 22 through 26 indicate the the appearance of filters collected at the Gamble Street site during an eruption. Photographs 22 through 24 were from a filter collected on August 19, 1992 when the atmospheric particle loading was $989\mu\text{g}/\text{m}^3$. Photographs 25 and 26 were taken from the sample collected on August 20, 1992 with an atmospheric loading of $446\mu\text{g}/\text{m}^3$. All of these photographs are at a magnification of 950X ($1/4\text{in.} = 6.7\mu\text{m}$). The source of most of this material is unquestionably Mount Spur ash. Photograph 22 as mentioned above contain a volcanic hematite crystal (A) but it also contains microlithic glass (B), feldspar (C), and magnetite particles (D). Photograph 23 is dominated by microlithic volcanic glass (A) characteristic of the standard sample of Mount Spur ash shown in photograph 4. Photograph 24 illustrates the magnetic properties of magnetite and related iron oxides (A). This photograph is of a special mount that was made and then exposed to a

magnetic field. All the iron oxide particles aligned themselves with the magnetic field. Photograph 25 and 26 are from the standard mount (not exposed to a magnetic field). Photograph 25 is a classic Mount Spur ash assemblage with the microlithic glass (A) and magnetite particles (B). Shards of volcanic glass are also present in this photograph (C). Photograph 26 contains an asphaltic concrete particle (A) along with the volcanic glass (B) and magnetite (C).

Photographs 27 and 28 are from the filter dated April 8, 1993. These two photographs are of the same field of view but at different focal depths in the mount. The magnification in the photographs is 950X. The atmospheric loading when this sample was collected was $171\mu\text{g}/\text{m}^3$. Photograph 27 is focused on a large fragment of shell (A) typical of those found in the road sand used on the roads during the winter of '93/'94. Rounded mineral grains (B) were also common both in this sample and in the road sand. Focusing below the shell particle, photograph 28, there are additional rounded grains (A), tire wear (B), and significant amounts of Mount Spur magnetite filled volcanic glass (C) that has been rounded from weathering and exposure, and feldspar (D). The Mount Spur eruption deposited a significant amount of ash on the Anchorage area. The original source of the magnetite filled volcanic glass is not in question but the mechanism of its secondary suspension is (see Discussion section below).

Photographs 29 through 32 are from the filter dated November 4, 1993. The airborne particle loading on this date was $161\mu\text{g}/\text{m}^3$. Photograph 29 was taken at a magnification of 237X. It shows a typical traffic debris assemblage of tire wear (A), asphaltic concrete (B), a cenosphere (C), and rounded mineral grains (D). At higher magnification, 950X, photograph 30 shows a tire wear particle (A) with quartz filler (B) and an asphaltic concrete particle (C). Photograph 31, taken at 950X, has a shell fragment in the center of the frame (A), a small microlithic glass particle (B), rounded mineral grain (C), and a magnetite particle (D). Photograph 32 shows the persistence of the Mount Spur microlithic volcanic glass (A). This field of view also contains a small tire wear particle (B), a magnetite particle (C), a rounded glass covered pyroxene (D), and a feldspar particle (E). Photograph 32 was taken at a magnification of 950X. The November 4, 1994 sample contains road sand, traffic debris, and rounded Mount Spur ash assemblages.

Photographs 33 and 34 were taken at a magnification of 950X and are both from the filter dated February 14, 1994. Photograph 33 shows a large shell fragment (A), an asphaltic particle (B), rounded minerals (C), tire wear particle (D), and magnetite (E). Photograph 34 contains the image of a tire wear particle (A), a picrolite lath (B), feldspar grains (C), and well rounded volcanic glass (D). The shell fragment and the picrolite lath are both materials found in the road sand used on the roads during the winter of '93/'94. This sample was dominated by road sand and traffic debris assemblages.

DISCUSSION

The process of quantifying source contributions, receptor source apportionment, requires a method of quantification that is normalized across the samples analyzed and a characterization of the sources involved relative to the factors quantified. The method used

to normalize the results from sample to sample in this analysis was to relate the opaque fraction and the crystalline fraction to the total detected material in a given field of view. Within a series of analyses this is a reasonable approach but from one series to another it is subject to error due to the fact that the method used to determine the total particle concentration, darkfield microscopy, is the most subject to error. The error is due to the level set as the threshold for determining the edge of the particle. Once a threshold is selected the results are relatively uniform for a series of analyses but between different series the results may be skewed as a result of differences in the darkfield threshold selected.

There are two series of analyses represented in this study. The first series was analyzed in 1990 and consisted of four samples: April 22, 1989 and April 7, 9, and 11, 1990. The second series involved nine samples: April 4, 1989; September 8, 1989; April 5, 7, 8, and 9, 1993; November 4, 1993; and February 14, 1994. For the purpose of this study five more samples were added to better characterize the variability in the Anchorage suspended particle population: April 12, 1989; July 1, 1992; August 13, 19, and 20, 1992. All eighteen of these samples have been examined in detail as part of this most recent study. Two issues become apparent. The first is that identifying the source assemblages that contribute to a particle population is based on features that do not lend themselves to instrumental analysis procedures. The second is that the point at which the resuspension of volcanic ash becomes a controllable event is not defined by any particle attribute. The first issue is resolved by using qualitative and semi-quantitative methods to establish the assemblages that are present and then applying the quantitative results for the sample and for each assemblage (see Table 1, page 7 of this report) to estimate the relative contribution of each source to the sample in question. The resultant values are then evaluated based on a reexamination of the samples. If there is no obvious inconsistency the values stand. If there is an inconsistency the values are adjusted to be consistent with visual and calculated results.

SAMPLE DATE	PM10 Loading	Assem. Ranking (%)
April 4, 1989	80 $\mu\text{g}/\text{m}^3$	Traffic, Sand
April 12, 1989	91 $\mu\text{g}/\text{m}^3$	Traffic (57%), Sand (43%)
April 22, 1989	50 $\mu\text{g}/\text{m}^3$	Traffic (100%)
Sept. 8, 1989	33 $\mu\text{g}/\text{m}^3$	Natural (78%), Traffic (22%)
April 7, 1990	152 $\mu\text{g}/\text{m}^3$	Ash (40%), Traffic (40%), Sand (20%)
April 9, 1990	188 $\mu\text{g}/\text{m}^3$	Ash (45%), Sand (28%), Traffic (27%)
April 11, 1990	260 $\mu\text{g}/\text{m}^3$	Ash (50%), Sand (30%), Traffic (20%)
July 1, 1992	47 $\mu\text{g}/\text{m}^3$	Traffic (100%)
Aug. 13, 1992	31 $\mu\text{g}/\text{m}^3$	Traffic (80%), Natural (20%)
Aug. 19, 1992	989 $\mu\text{g}/\text{m}^3$	Ash (95%), Traffic (5%)
Aug. 20, 1992	446 $\mu\text{g}/\text{m}^3$	Ash (87%), Traffic (12%), Natural (1%)
April 5, 1993	164 $\mu\text{g}/\text{m}^3$	Sand (55%), Traffic (25%), Ash (20%)
April 7, 1993	185 $\mu\text{g}/\text{m}^3$	Sand (45%), Traffic (35%), Ash (20%)
April 7, 1993	Collocated Sample	Sand, Traffic, Ash
April 8, 1993	171 $\mu\text{g}/\text{m}^3$	Sand (40%), Traffic (38%), Ash (22%)
April 9, 1993	162 $\mu\text{g}/\text{m}^3$	Sand (40%), Ash (30%), Traffic (30%)
Nov. 4, 1993	161 $\mu\text{g}/\text{m}^3$	Traffic (48%), Sand (32%), Ash (20%)
Feb. 14, 1994	242 $\mu\text{g}/\text{m}^3$	Sand (40%), Traffic (36%), Ash (24%)

The second issue is more difficult. The 1993 samples contain significant amounts of Mount Spur ash but the ash is obviously weathered and rounded. The source of much of this ash may be mud that is tracked out onto the road on tires. Much of the Mount Redoubt ash seen in the April 1990 samples was largely unweathered. The unweathered ash has not experienced processes that incorporate the ash into the soil. Following the Mount St. Helen eruption in Washington State it took nearly a year to stabilize the deposited ash.

CONCLUSION

The samples from April 1990 were strongly influenced by the Mount Redoubt ash fall. By 1992 no recent ash was evident in the samples until the eruption of Mount Spur, August 18, 1992. The large quantity of Mount Spur ash that fell on Anchorage has resulted in its persistent presence in the samples since that time. The Mount Spur ash in the April 1993 samples exhibits evidence of weathering, a process involved in incorporating the ash fall into the natural soil. The main contributors to the particle loading in April 1993 and since that time have been sand on the road and traffic debris.

Thank you for this opportunity to be of service. If I can provide any further assistance please contact me.

Signed: 
E. R. Crutcher, Consultant

Table of Photographs

- Photograph 1: Mount Redoubt Volcanic Ash Fall from the Eruption of December 21, 1989 Collected in Anchorage, Alaska (Magnification: 237X, 15 degrees off crossed circular polarized light)
- Photograph 2: Mount Redoubt Volcanic Ash Fall from the Eruption of December 21, 1989 Collected in Anchorage, Alaska (Magnification: 950X, 15 degrees off crossed circular polarized light)
- Photograph 3: Mount Spur Volcanic Ash Fall from the Eruption of August 18, 1992 Collected in Anchorage, Alaska Crushed in the Laboratory for Analysis
(Magnification: 237X, 15 degrees off crossed circular polarized light)
- Photograph 4: Mount Spur Volcanic Ash Fall from the Eruption of August 18, 1992 Collected in Anchorage, Alaska Crushed in the Laboratory for Analysis
(Magnification: 950X, 15 degrees off crossed circular polarized light)
- Photograph 5: Road Sand Standard from the Stock Pile Used on the Roads of Anchorage, Alaska During the Winter of 1994, Crushed in the Laboratory for Analysis (Magnification: 95X, 15 degrees off crossed circular polarized light)
- Photograph 6: Road Sand Standard from the Stock Pile Used on the Roads of Anchorage, Alaska During the Winter of 1994, Crushed in the Laboratory for Analysis (Magnification: 237X, 15 degrees off crossed circular polarized light)
- Photograph 7: Road Sand Standard from the Stock Pile Used on the Roads of Anchorage, Alaska During the Winter of 1994, Crushed in the Laboratory for Analysis (Magnification: 950X, 15 degrees off crossed circular polarized light)

- Photograph 8: Road Sand Standard from the Stock Pile Used on the Roads of Anchorage, Alaska During the Winter of 1994,
Crushed in the Laboratory for Analysis (Magnification: 950X, 15 degrees off crossed circular polarized light)
- Photograph 9: High Volume Filter Sample, Anchorage, Alaska, September 8, 1989, Site: ERPG-A,
Loading: $33\mu\text{g}/\text{M}^3$ (Magnification: 950X)
- Photograph 10: High Volume Filter Sample, Anchorage, Alaska, April 4, 1989, Site: Gamble N.,
Loading: $80\mu\text{g}/\text{M}^3$ (Magnification: 950X, 15 degrees off crossed circular polarized light)
- Photograph 11: High Volume Filter Sample, Anchorage, Alaska, April 12, 1989, Site: Gamble,
Loading: $91\mu\text{g}/\text{M}^3$ (Magnification: 475X, 15 degrees off crossed circular polarized light)
- Photograph 12: High Volume Filter Sample, Anchorage, Alaska, April 12, 1989, Site: Gamble,
Loading: $91\mu\text{g}/\text{M}^3$ (Magnification: 950X, 15 degrees off crossed circular polarized light)
- Photograph 13: High Volume Filter Sample, Anchorage, Alaska, April 9, 1990, Site: Gamble,
Loading: $188\mu\text{g}/\text{M}^3$ (Magnification: 950X, 15 degrees off crossed circular polarized light)
- Photograph 14: High Volume Filter Sample, Anchorage, Alaska, April 9, 1990, Site: Gamble,
Loading: $188\mu\text{g}/\text{M}^3$ (Magnification: 950X, 15 degrees off crossed circular polarized light)
- Photograph 15: High Volume Filter Sample, Anchorage, Alaska, April 11, 1990, Site: Gamble,
Loading: $260\mu\text{g}/\text{M}^3$ (Magnification: 950X, 15 degrees off crossed circular polarized light)
- Photograph 16: High Volume Filter Sample, Anchorage, Alaska, April 11, 1990, Site: Gamble,
Loading: $260\mu\text{g}/\text{M}^3$ (Magnification: 950X, 15 degrees off crossed circular polarized light)
- Photograph 17: High Volume Filter Sample, Anchorage, Alaska, August 13, 1992, Site: Gamble,
Loading: $31\mu\text{g}/\text{M}^3$ (Magnification: 475X, 15 degrees off crossed circular polarized light)
- Photograph 18: High Volume Filter Sample, Anchorage, Alaska, August 13, 1992, Site: Gamble,
Loading: $31\mu\text{g}/\text{M}^3$ (Magnification: 950X, 15 degrees off crossed circular polarized light)
- Photograph 19: High Volume Filter Sample, Anchorage, Alaska, August 13, 1992, Site: Gamble,
Loading: $31\mu\text{g}/\text{M}^3$ (Magnification: 950X)
- Photograph 20: High Volume Filter Sample, Anchorage, Alaska, August 13, 1992, Site: Gamble,
Loading: $31\mu\text{g}/\text{M}^3$ (Magnification: 950X, 15 degrees off crossed circular polarized light)
- Photograph 21: High Volume Filter Sample, Anchorage, Alaska, August 13, 1992, Site: Gamble,
Loading: $31\mu\text{g}/\text{M}^3$ (Magnification: 950X, 15 degrees off crossed circular polarized light)
- Photograph 22: High Volume Filter Sample, Anchorage, Alaska, August 19, 1992, Site: Gamble,
Loading: $989\mu\text{g}/\text{M}^3$ (Magnification: 950X, 15 degrees off crossed circular polarized light)
- Photograph 23: High Volume Filter Sample, Anchorage, Alaska, August 19, 1992, Site: Gamble,
Loading: $989\mu\text{g}/\text{M}^3$ (Magnification: 950X)
- Photograph 24: High Volume Filter Sample, Anchorage, Alaska, August 19, 1992, Site: Gamble,
Loading: $989\mu\text{g}/\text{M}^3$ (Magnification: 950X)
- Photograph 25: High Volume Filter Sample, Anchorage, Alaska, August 20, 1992, Site: Gamble,
Loading: $446\mu\text{g}/\text{M}^3$ (Magnification: 950X)
- Photograph 26: High Volume Filter Sample, Anchorage, Alaska, August 20, 1992, Site: Gamble,
Loading: $446\mu\text{g}/\text{M}^3$ (Magnification: 950X)
- Photograph 27: High Volume Filter Sample, Anchorage, Alaska, April 8, 1993, Site: Gamble 26C,
Loading: $171\mu\text{g}/\text{M}^3$ (Magnification: 950X, 15 degrees off crossed circular polarized light)
- Photograph 28: High Volume Filter Sample, Anchorage, Alaska, April 8, 1993, Site: Gamble 26C,
Loading: $171\mu\text{g}/\text{M}^3$ (Magnification: 950X, 15 degrees off crossed circular polarized light)
- Photograph 29: High Volume Filter Sample, Anchorage, Alaska, November 4, 1993, Site: Gamble 26C,
Loading: $161\mu\text{g}/\text{M}^3$ (Magnification: 237X, 15 degrees off crossed circular polarized light)
- Photograph 30: High Volume Filter Sample, Anchorage, Alaska, November 4, 1993, Site: Gamble 26C,
Loading: $161\mu\text{g}/\text{M}^3$ (Magnification: 950X, 15 degrees off crossed circular polarized light)
- Photograph 31: High Volume Filter Sample, Anchorage, Alaska, November 4, 1993, Site: Gamble 26C,
Loading: $161\mu\text{g}/\text{M}^3$ (Magnification: 950X, 15 degrees off crossed circular polarized light)
- Photograph 32: High Volume Filter Sample, Anchorage, Alaska, November 4, 1993, Site: Gamble 26C,
Loading: $161\mu\text{g}/\text{M}^3$ (Magnification: 950X, 15 degrees off crossed circular polarized light)
- Photograph 33: High Volume Filter Sample, Anchorage, Alaska, February 14, 1994, Site: Gamble 26C,
Loading: $242\mu\text{g}/\text{M}^3$ (Magnification: 950X, 15 degrees off crossed circular polarized light)
- Photograph 34: High Volume Filter Sample, Anchorage, Alaska, February 14, 1994, Site: Gamble 26C,
Loading: $242\mu\text{g}/\text{M}^3$ (Magnification: 950X, 15 degrees off crossed circular polarized light)



Photograph 1: Mount Redoubt Volcanic Ash Fall from the Eruption of December 21, 1989 Collected in Anchorage, Alaska (Magnification: 237X, 15 degrees off crossed circular polarized light)

A = feldspar
B = pyroxenes
C = Vol. glass
D = background
E = glass foam



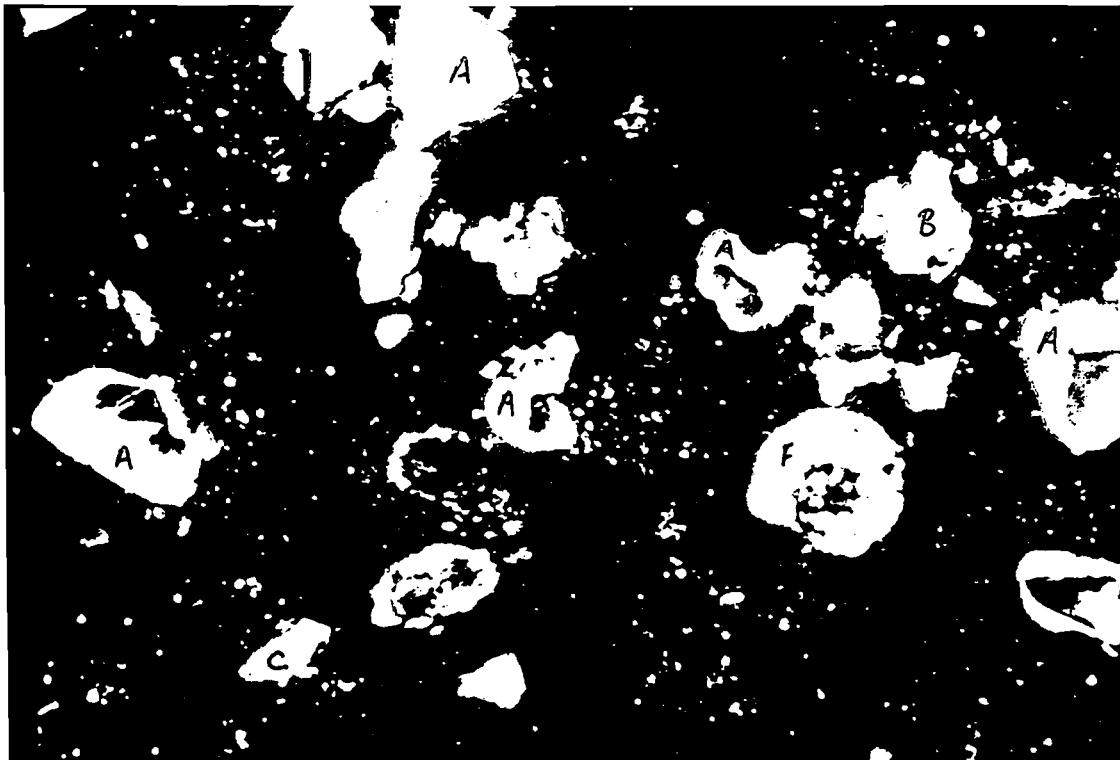
Photograph 2: Mount Redoubt Volcanic Ash Fall from the Eruption of December 21, 1989 Collected in Anchorage, Alaska (Magnification: 950X, 15 degrees off crossed circular polarized light)



Photograph 3: Mount Spur Volcanic Ash Fall from the Eruption of August 18, 1992 Collected in Anchorage, Alaska Crushed in the Laboratory for Analysis
(Magnification: 237X, 15 degrees off crossed circular polarized light)



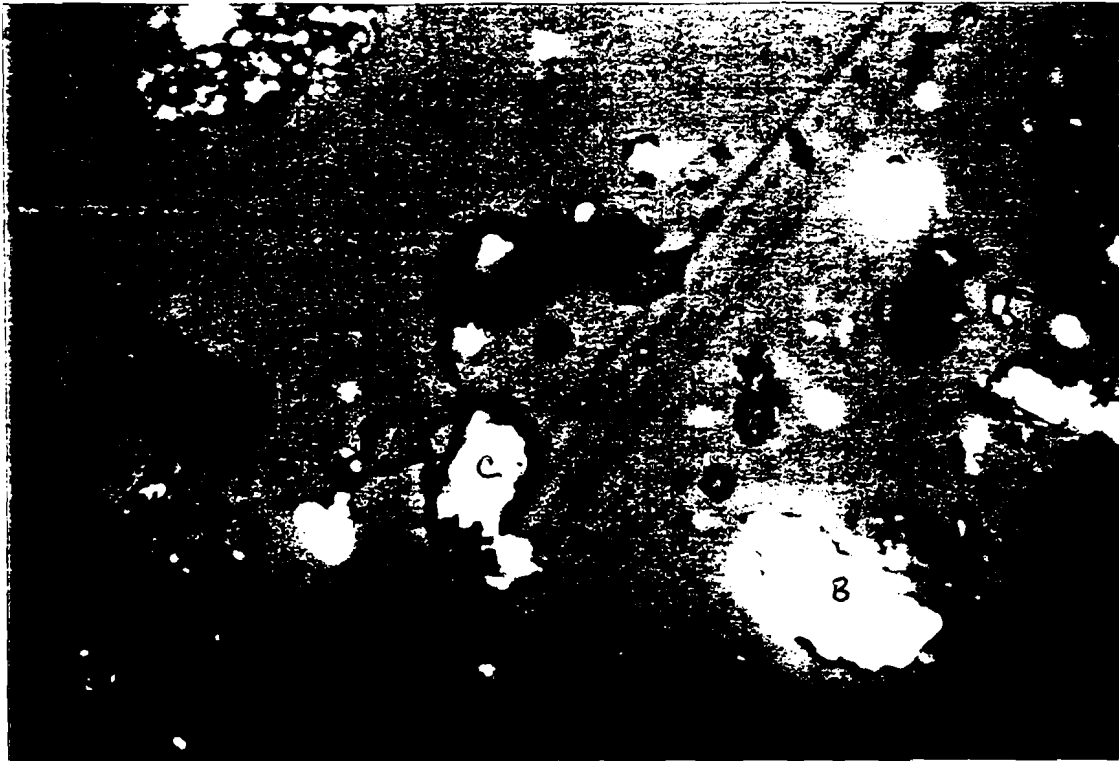
Photograph 4: Mount Spur Volcanic Ash Fall from the Eruption of August 18, 1992 Collected in Anchorage, Alaska Crushed in the Laboratory for Analysis
(Magnification: 950X, 15 degrees off crossed circular polarized light)



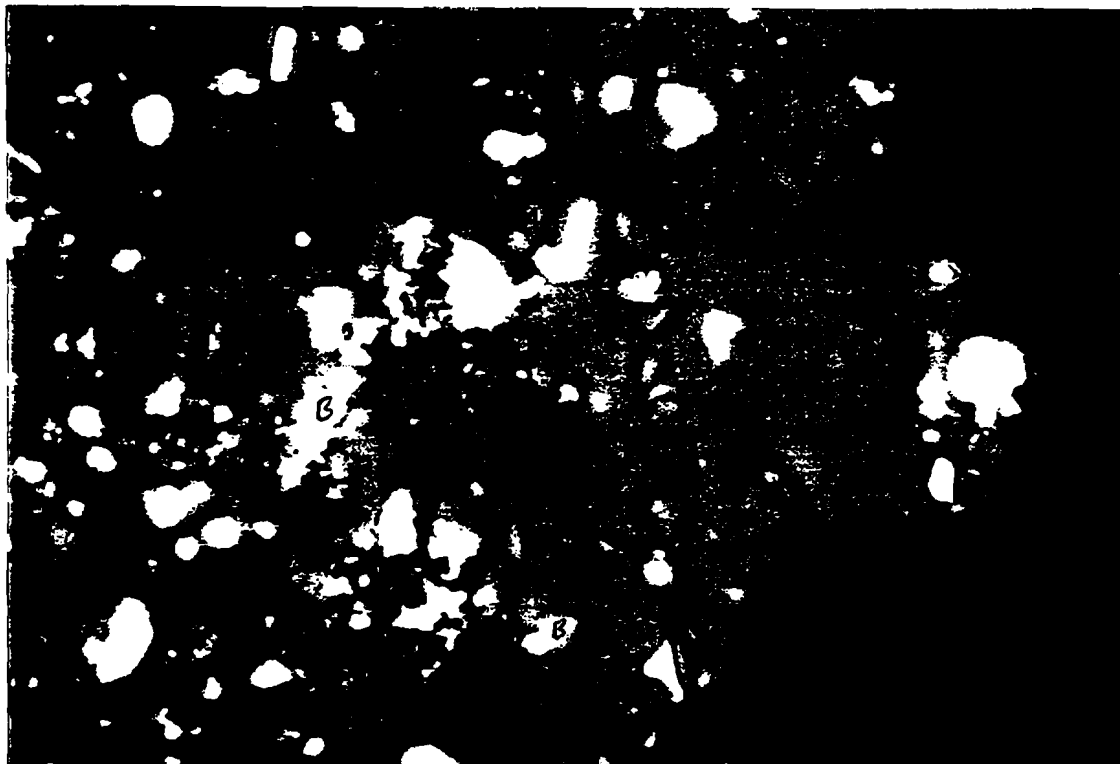
Photograph 5: Road Sand Standard from the Stock Pile Used on the Roads of Anchorage, Alaska
During the Winter of 1994, Crushed in the Laboratory for Analysis
(Magnification: 95X, 15 degrees off crossed circular polarized light)



Photograph 6: Road Sand Standard from the Stock Pile Used on the Roads of Anchorage, Alaska
During the Winter of 1994, Crushed in the Laboratory for Analysis
(Magnification: 237X, 15 degrees off crossed circular polarized light)



Photograph 7: Road Sand Standard from the Stock Pile Used on the Roads of Anchorage, Alaska
During the Winter of 1994, Crushed in the Laboratory for Analysis
(Magnification: 950X, 15 degrees off crossed circular polarized light)



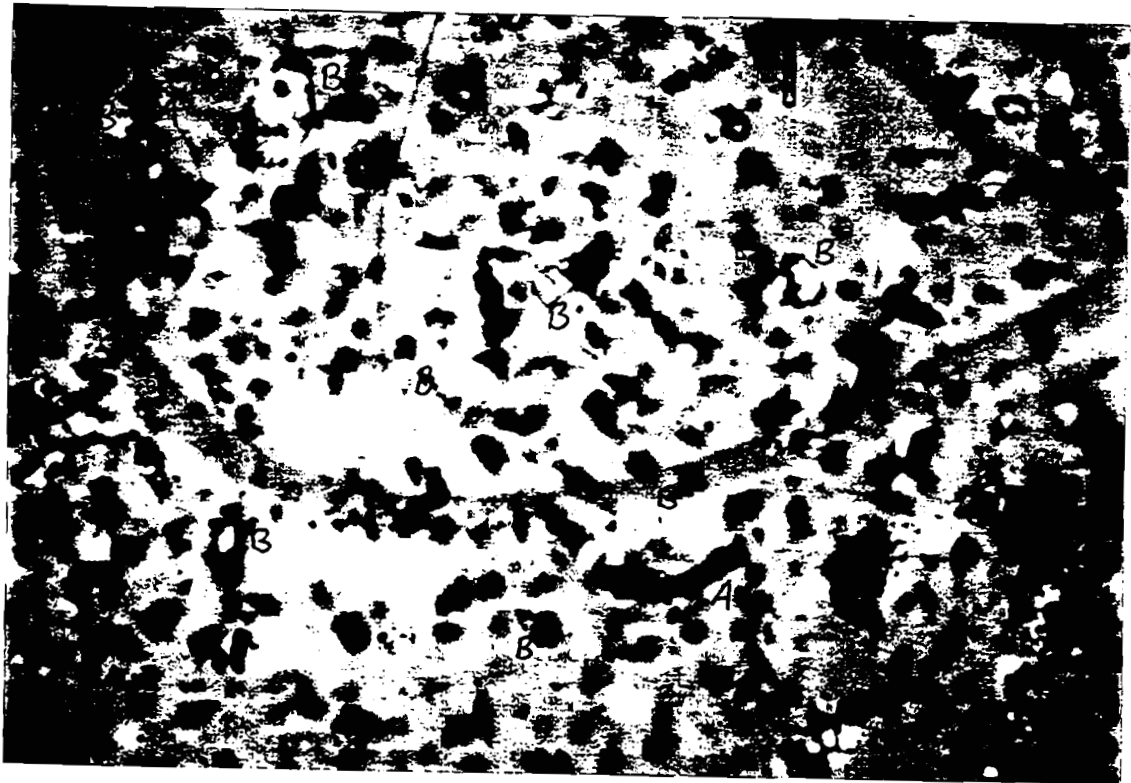
Photograph 8: Road Sand Standard from the Stock Pile Used on the Roads of Anchorage, Alaska
During the Winter of 1994, Crushed in the Laboratory for Analysis
(Magnification: 950X, 15 degrees off crossed circular polarized light)



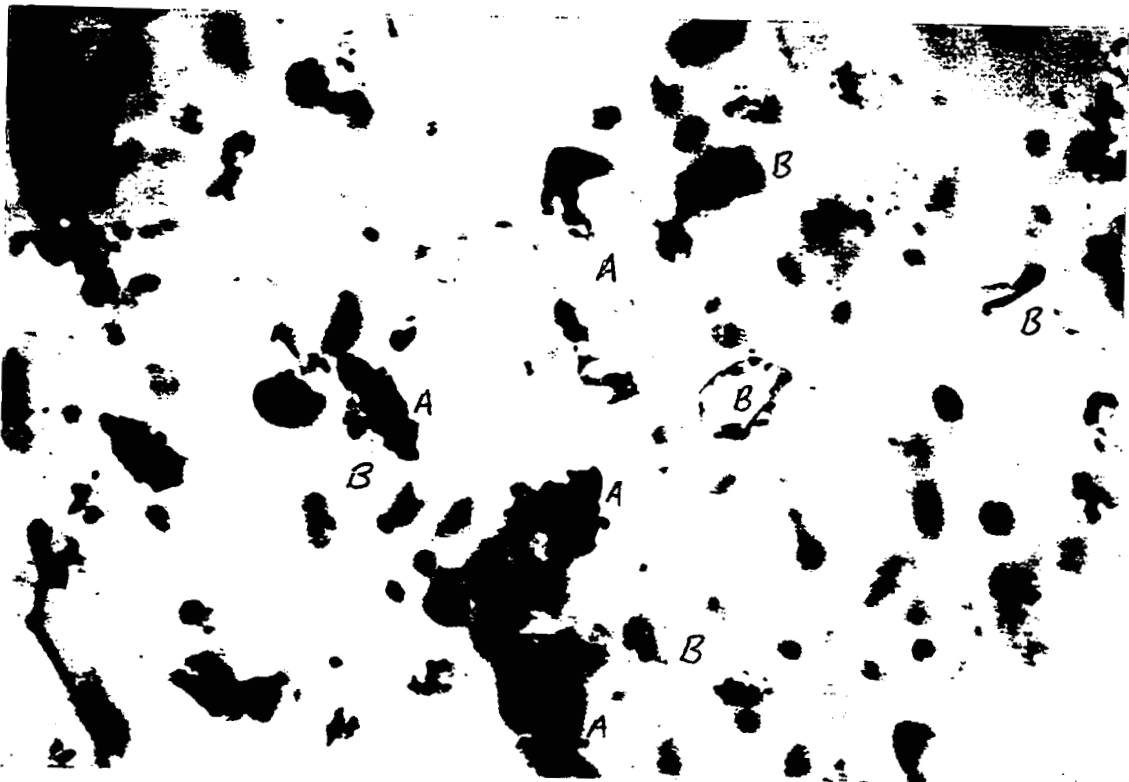
Photograph 9: High Volume Filter Sample, Anchorage, Alaska, September 8, 1989, Site: ERPG-A,
Loading: $33\mu\text{g}/\text{M}^3$ (Magnification: 950X)



Photograph 10: High Volume Filter Sample, Anchorage, Alaska, April 4, 1989, Site: Gamble N.,
Loading: $80\mu\text{g}/\text{M}^3$ (Magnification: 950X, 15 degrees off crossed circular polarized light)
237



Photograph 11: High Volume Filter Sample, Anchorage, Alaska, April 12, 1989, Site: Gamble,
Loading: $91\mu\text{g}/\text{M}^3$ (Magnification: 475X, 15 degrees off crossed circular polarized light)



Photograph 12: High Volume Filter Sample, Anchorage, Alaska, April 12, 1989, Site: Gamble,
Loading: $91\mu\text{g}/\text{M}^3$ (Magnification: 950X, 15 degrees off crossed circular polarized light)



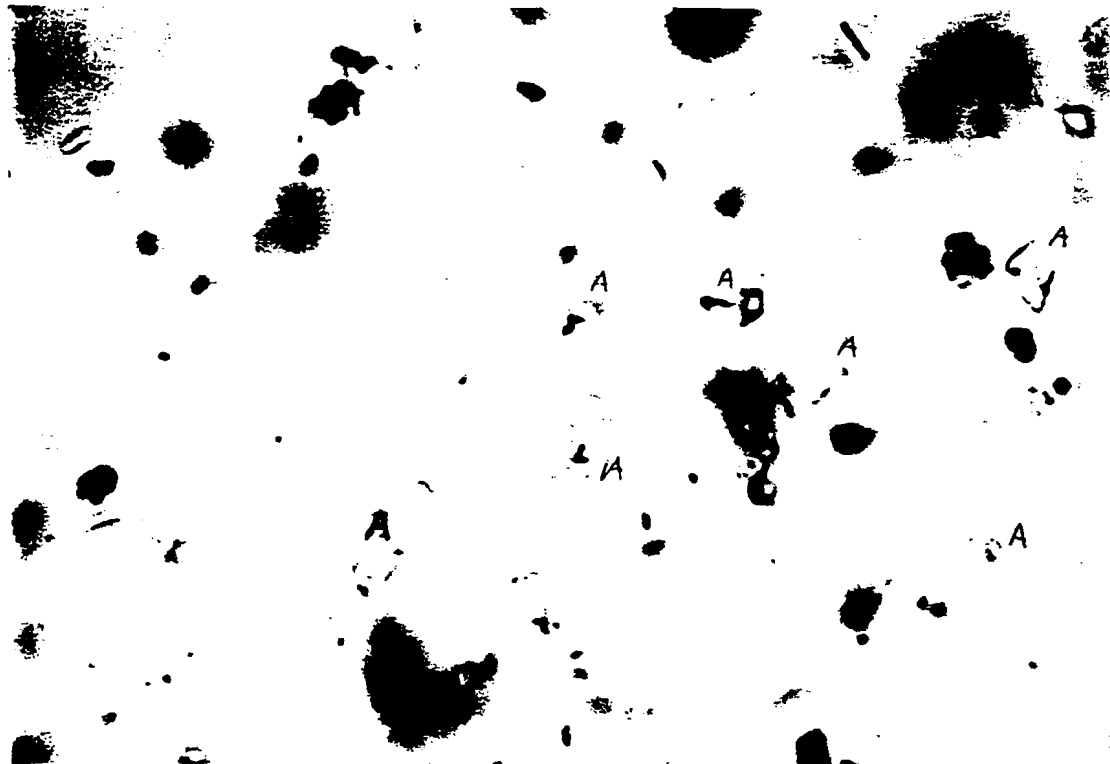
Photograph 13: High Volume Filter Sample, Anchorage, Alaska, April 9, 1990, Site: Gamble,
Loading: $188\mu\text{g}/\text{M}^3$ (Magnification: 950X, 15 degrees off crossed circular polarized light)



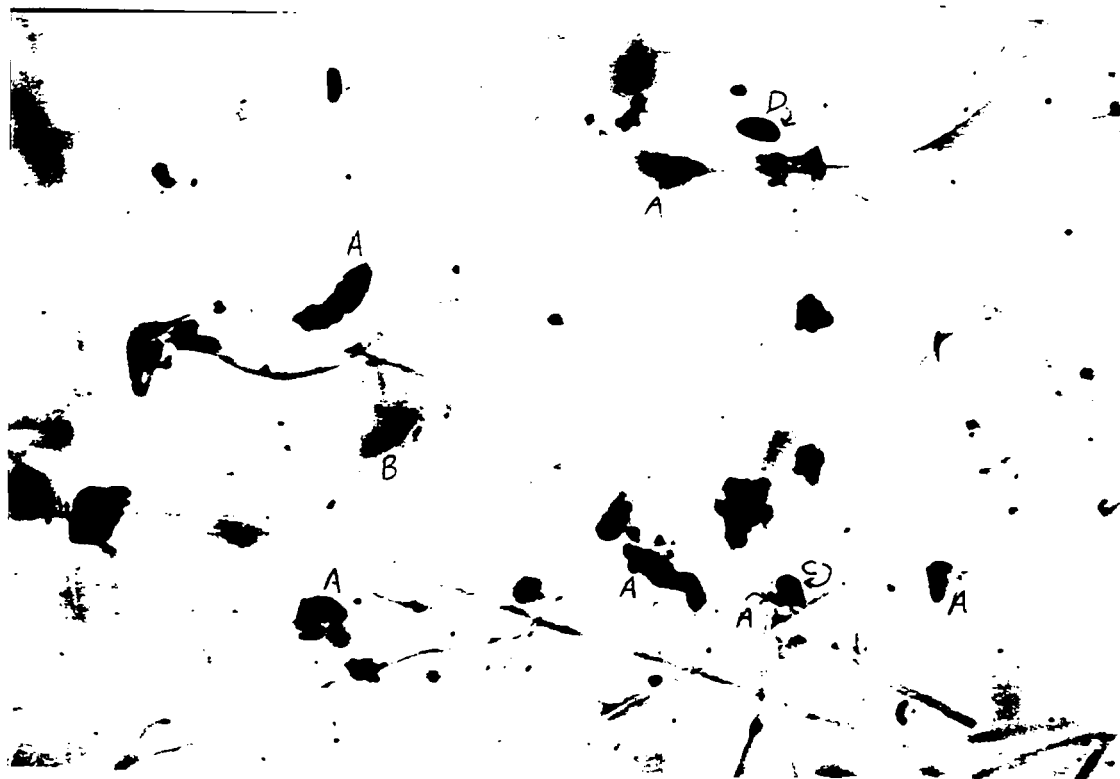
Photograph 14: High Volume Filter Sample, Anchorage, Alaska, April 9, 1990, Site: Gamble,
Loading: $188\mu\text{g}/\text{M}^3$ (Magnification: 950X, 15 degrees off crossed circular polarized light)



Photograph 15: High Volume Filter Sample, Anchorage, Alaska, April 11, 1990, Site: Gamble,
Loading: $260\mu\text{g}/\text{M}^3$ (Magnification: 950X, 15 degrees off crossed circular polarized light)



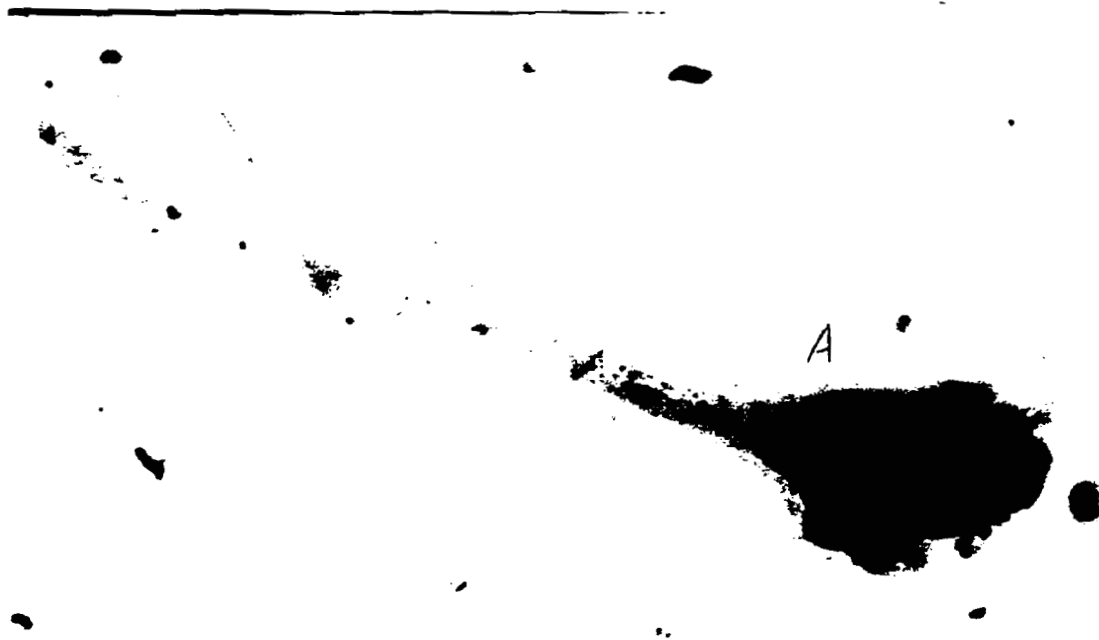
Photograph 16: High Volume Filter Sample, Anchorage, Alaska, April 11, 1990, Site: Gamble,
Loading: $260\mu\text{g}/\text{M}^3$ (Magnification: 950X, 15 degrees off crossed circular polarized light)



Photograph 17: High Volume Filter Sample, Anchorage, Alaska, August 13, 1992, Site: Gamble,
Loading: $31\mu\text{g}/\text{M}^3$ (Magnification: 475X, 15 degrees off crossed circular polarized light)



Photograph 18: High Volume Filter Sample, Anchorage, Alaska, August 13, 1992, Site: Gamble,
Loading: $31\mu\text{g}/\text{M}^3$ (Magnification: 950X, 15 degrees off crossed circular polarized light)



Photograph 19: High Volume Filter Sample, Anchorage, Alaska, August 13, 1992, Site: Gamble,
Loading: $31\mu\text{g}/\text{M}^3$ (Magnification: 950X)



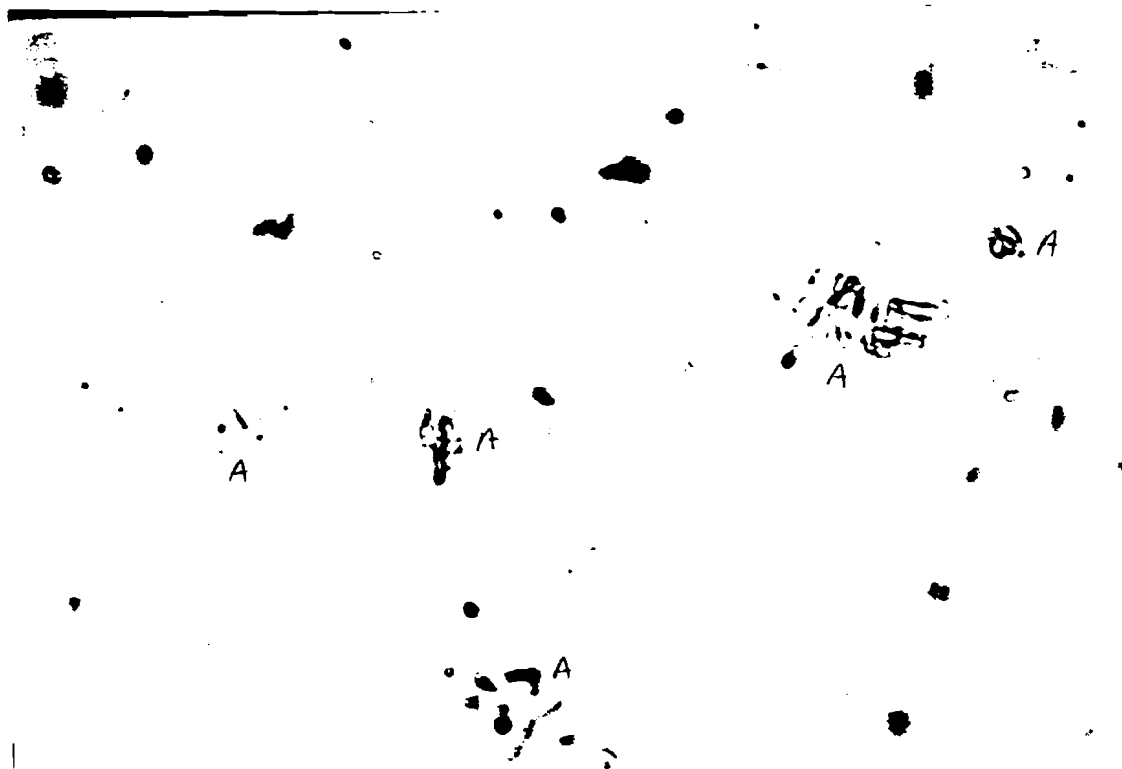
Photograph 20: High Volume Filter Sample, Anchorage, Alaska, August 13, 1992, Site: Gamble,
Loading: $31\mu\text{g}/\text{M}^3$ (Magnification: 950X, 15 degrees off crossed circular polarized light)



Photograph 21: High Volume Filter Sample, Anchorage, Alaska, August 13, 1992, Site: Gamble,
Loading: $31\mu\text{g}/\text{M}^3$ (Magnification: 950X, 15 degrees off crossed circular polarized light)



Photograph 22: High Volume Filter Sample, Anchorage, Alaska, August 19, 1992, Site: Gamble,
Loading: $989\mu\text{g}/\text{M}^3$ (Magnification: 950X, 15 degrees off crossed circular polarized light)



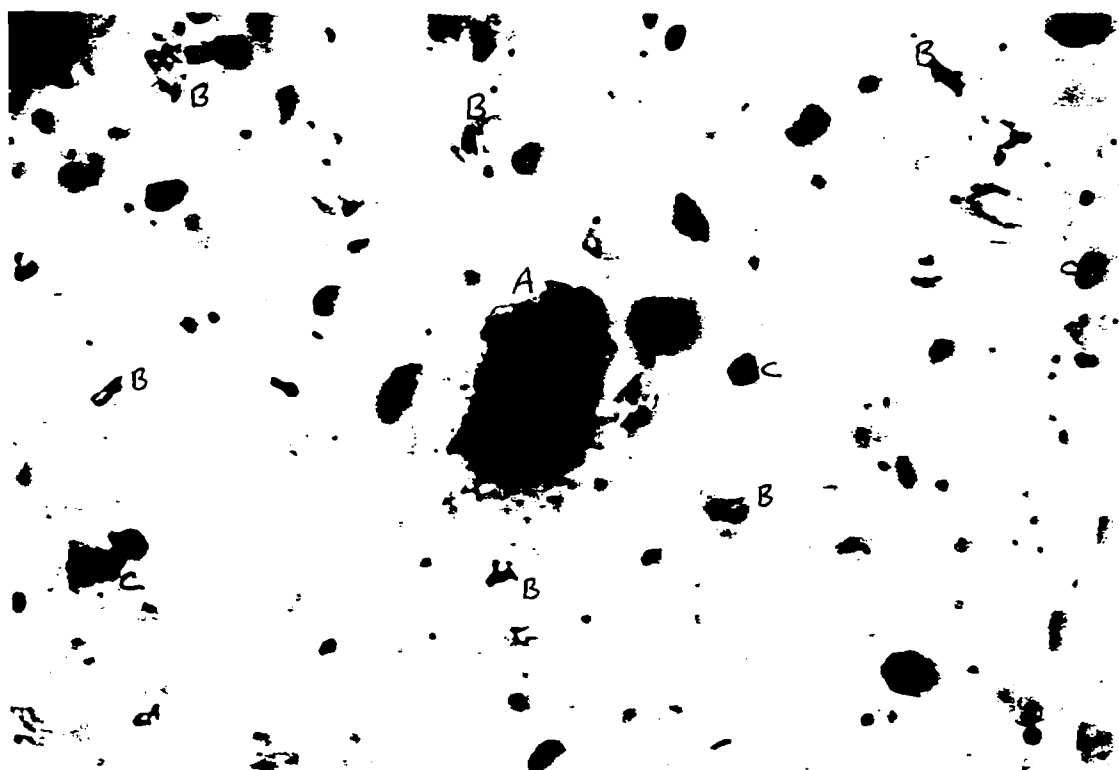
Photograph 23: High Volume Filter Sample, Anchorage, Alaska, August 19, 1992, Site: Gamble,
Loading: $989\mu\text{g}/\text{M}^3$ (Magnification: 950X)



Photograph 24: High Volume Filter Sample, Anchorage, Alaska, August 19, 1992, Site: Gamble,
Loading: $989\mu\text{g}/\text{M}^3$ (Magnification: 950X)



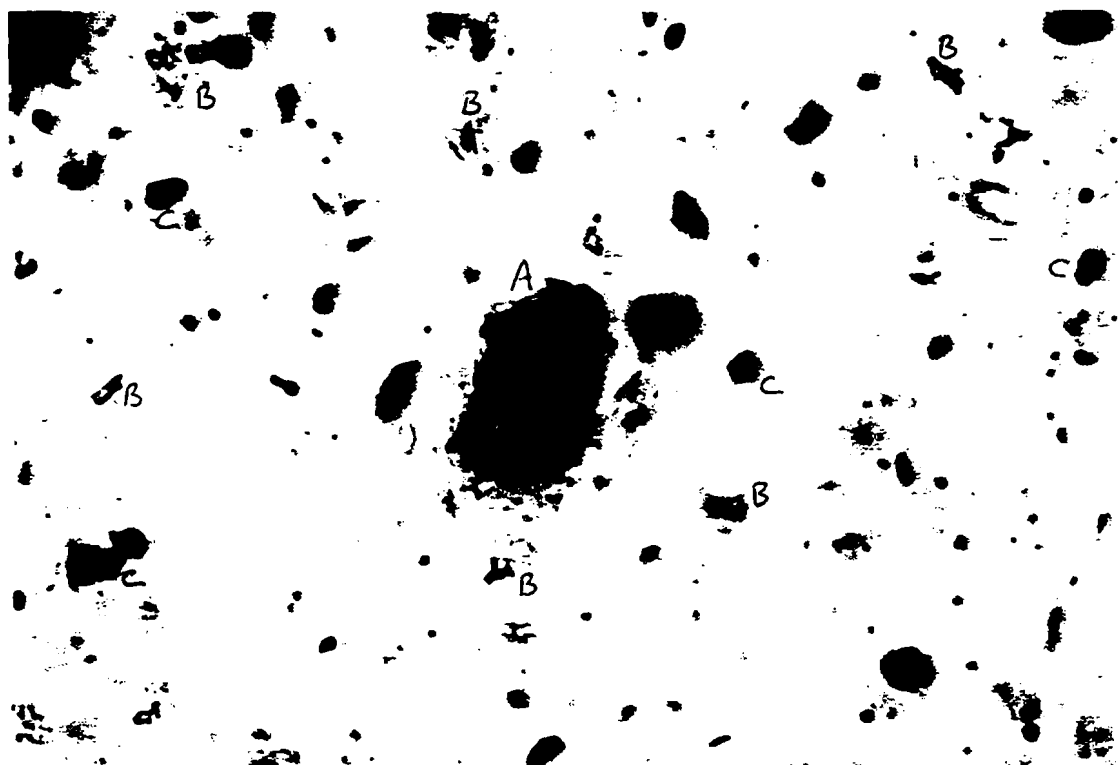
Photograph 25: High Volume Filter Sample, Anchorage, Alaska, August 20, 1992, Site: Gamble,
Loading: $446\mu\text{g}/\text{M}^3$ (Magnification: 950X)



Photograph 26: High Volume Filter Sample, Anchorage, Alaska, August 20, 1992, Site: Gamble,
Loading: $446\mu\text{g}/\text{M}^3$ (Magnification: 950X)



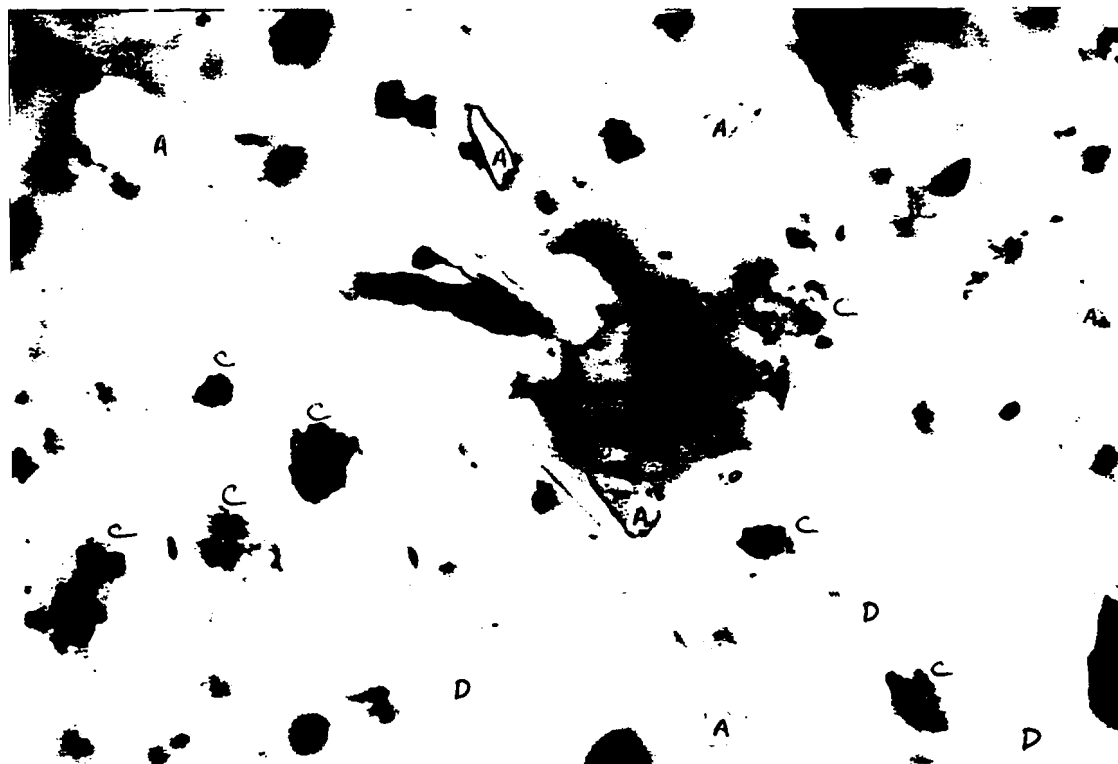
Photograph 25: High Volume Filter Sample, Anchorage, Alaska, August 20, 1992, Site: Gamble,
Loading: $446\mu\text{g}/\text{M}^3$ (Magnification: 950X)



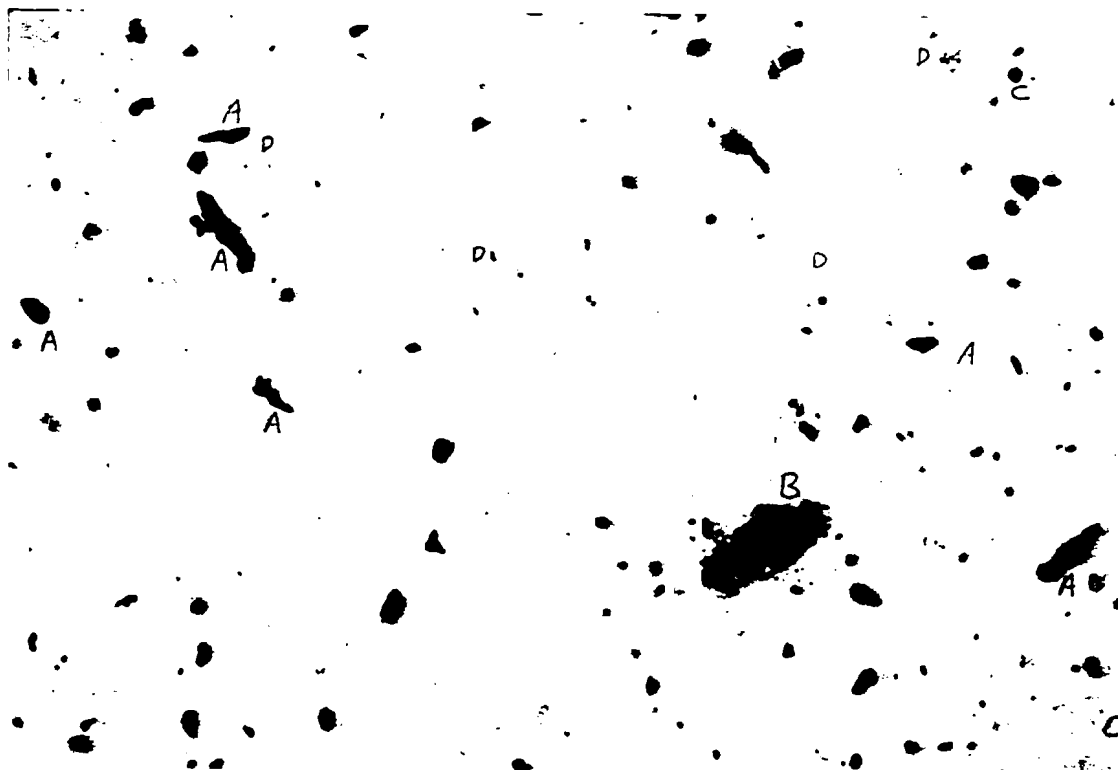
Photograph 26: High Volume Filter Sample, Anchorage, Alaska, August 20, 1992, Site: Gamble,
Loading: $446\mu\text{g}/\text{M}^3$ (Magnification: 950X)



Photograph 27: High Volume Filter Sample, Anchorage, Alaska, April 8, 1993, Site: Gamble 26C,
Loading: $171\mu\text{g}/\text{M}^3$ (Magnification: 950X, 15 degrees off crossed circular polarized light)



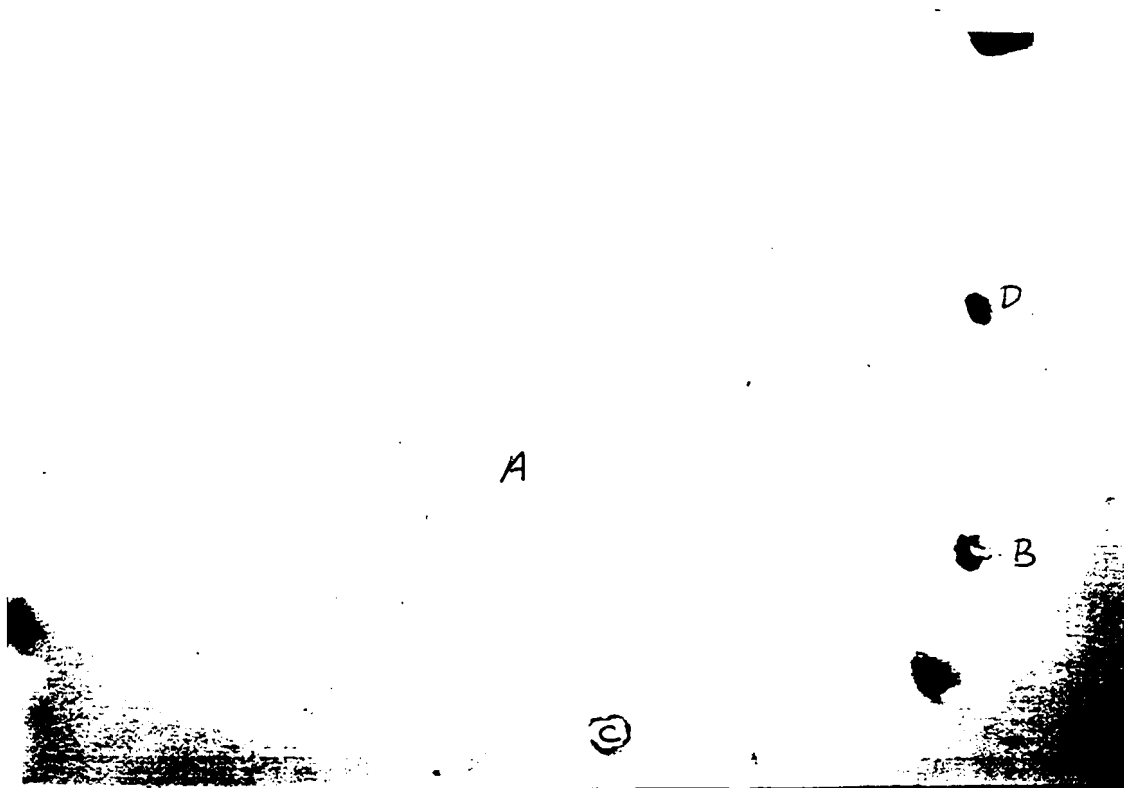
Photograph 28: High Volume Filter Sample, Anchorage, Alaska, April 8, 1993, Site: Gamble 26C,
Loading: $171\mu\text{g}/\text{M}^3$ (Magnification: 950X, 15 degrees off crossed circular polarized light)



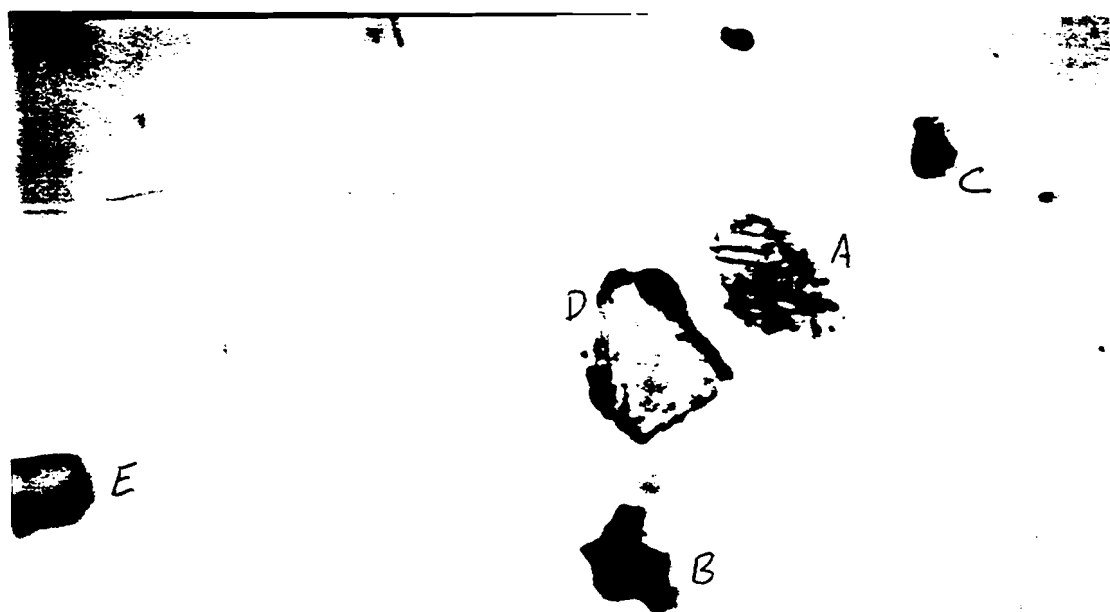
Photograph 29: High Volume Filter Sample, Anchorage, Alaska, November 4, 1993, Site: Gamble 26C,
Loading: $161\mu\text{g}/\text{M}^3$ (Magnification: 237X, 15 degrees off crossed circular polarized light)



Photograph 30: High Volume Filter Sample, Anchorage, Alaska, November 4, 1993, Site: Gamble 26C,
Loading: $161\mu\text{g}/\text{M}^3$ (Magnification: 950X, 15 degrees off crossed circular polarized light)



Photograph 31: High Volume Filter Sample, Anchorage, Alaska, November 4, 1993, Site: Gamble 26C,
Loading: $161 \mu\text{g}/\text{M}^3$ (Magnification: 950X, 15 degrees off crossed circular polarized light)



Photograph 32: High Volume Filter Sample, Anchorage, Alaska, November 4, 1993, Site: Gamble 26C,
Loading: $161 \mu\text{g}/\text{M}^3$ (Magnification: 950X, 15 degrees off crossed circular polarized light)



Photograph 33: High Volume Filter Sample, Anchorage, Alaska, February 14, 1994, Site: Gamble 26C,
Loading: $242\mu\text{g}/\text{M}^3$ (Magnification: 950X, 15 degrees off crossed circular polarized light)



Photograph 34: High Volume Filter Sample, Anchorage, Alaska, February 14, 1994, Site: Gamble 26C,
Loading: $242\mu\text{g}/\text{M}^3$ (Magnification: 950X, 15 degrees off crossed circular polarized light)

CALCULATIONS

ASSUMPTIONS:

1. Traffic Debris assemblage is at a nominal value of about $50\mu\text{g}/\text{m}^3$

This is based on the calculated values for the opaque fraction for a number of samples (fraction X Loading).

2. On days with high mineral loading the tire wear total mass increased.

On very low loading days the traffic debris assemblage dominated. On high loading days the traffic debris assemblage often increased in mass though its fraction of the total decreased (based on Fraction X Loading). The increase was presumably due to increased tire wear.

April 12, 1989 (in all equation x =percent traffic assemblage)

$$48 = x(77) + (1-x)(10), 38=67x, x=57, \text{ Sand} = 43$$

April 22, 1989

Essentially 100% traffic debris

September 8, 1989

$$15=x(77) + (1-x)(10), 5=67x, x=7.5, \text{ spores very low density, } 1/3 \text{ traffic debris density} \\ \text{mass } x=22.5=22, \text{ Natural} = 78$$

April 7, 1990

$$44=x(77) + (1-x)(20) \text{ maximum ash, } 24=57x, x=42, \text{ elevated traffic mass loading} \\ 44=x(77) + y(20) + (1-x-y)(10) \text{ isotropic correction for ash and sand contribution} \\ 40\% \text{ ash, } 40\% \text{ traffic, and } 20\% \text{ sand} = 40.8\% \text{ opaque, within } 10\% \text{ of reported value} \\ \text{and consistent with semi-quant assemblage analysis.}$$

April 9, 1990

$$36= x(77) + (1-x)(20), 16=57x, x=28 \\ 36=x(77) + y(20) + (1-x-y)(10) \text{ isotropic correction for ash and sand contribution} \\ 45\% \text{ ash, } 27\% \text{ traffic, and } 28\% \text{ sand} = 32.6\% \text{ opaque, within } 10\% \text{ of reported value} \\ \text{and consistent with semi-quant assemblage analysis.}$$

April 11, 1990

$30 = x(77) + (1-x)(20)$, $10 = 57x$, $x = 18$
 $30 = x(77) + y(20) + (1-x-y)(10)$ isotropic correction for ash and sand contribution
 50% ash, 20% traffic, and 30% sand = 28.4% opaque, within 10% of reported value
 and consistent with semi-quant assemblage analysis.

April 5, 1993 (Change to Mount Spur Ash with Opaques of 30%)

$13 = x(77) + (1-x)(10)$, $3 = 67x$, $x = 4.5\%$, mass of $7\mu\text{g}/\text{m}^3$ to low, adjust to $50\mu\text{g}/\text{m}^3$
 opaque percent must be 30
 $30 = x(77) + (1-x)(10)$, $20 = 67x$, $x = 29.8$
 $13 = x(77) + y(30) + (1-x-y)(10)$ isotropic correction for ash and sand contribution
 20% ash, 25% traffic, and 55% sand = 30.75% opaque, within 10% of reported value
 and consistent with semi-quant assemblage analysis.

April 7, 1993

Opaques of 17 normalized to sample of April 5, 1993: = 39
 $39 = x(77) + (1-x)(10)$
 $39 = x(77) + y(30) + (1-x-y)(10)$ isotropic correction for ash and sand contribution
 20% ash, 35% traffic, and 45% sand = 37.45% opaque, within 10% of reported value
 and consistent with semi-quant assemblage analysis.

April 8, 1993

Opaques of 18 normalized to sample of April 5, 1993: = 41.5
 $41 = x(77) + (1-x)(10)$
 $41 = x(77) + y(20) + (1-x-y)(10)$ isotropic correction for ash and sand contribution
 22% ash, 38% traffic, and 40% sand = 39.86% opaque, within 10% of reported value
 and consistent with semi-quant assemblage analysis.

April 9, 1993

Opaques of 15 normalized to sample of April 5, 1993: = 34.6
 $35 = x(77) + (1-x)(10)$
 $35 = x(77) + y(20) + (1-x-y)(10)$ isotropic correction for ash and sand contribution
 30% ash, 30% traffic, and 40% sand = 36.1% opaque, within 10% of reported value
 and consistent with semi-quant assemblage analysis.

November 4 1993

Opaques of 22 normalized to sample of April 5, 1993: = 50.77
 $51 = x(77) + (1-x)(10)$
 $51 = x(77) + y(20) + (1-x-y)(10)$ isotropic correction for ash and sand contribution
 20% ash, 48% traffic, and 32% sand = 46.2% opaque, within 10% of reported value
 and consistent with semi-quant assemblage analysis.

February 14, 1994

Opaques of 18 normalized to sample of April 5, 1993: = 41.5

$$41.5 = x(77) + (1-x)(10)$$

$41.5 = x(77) + y(20) + (1-x-y)(10)$ isotropic correction for ash and sand contribution
24% ash, 36% traffic, and 40% sand = 38.92% opaque, within 10% of reported value
and consistent with semi-quant assemblage analysis.

